PROCEEDINGS OF SCIENCE

The high temperature QCD static potential beyond leading order

Margaret E. Carrington,[a,b,*] **Cristina Manuel**[c,d] **and Joan Soto**[e,f]

[a] *Department of Physics, Brandon University, Brandon, Manitoba R7A 6A9, Canada*
[b] *Winnipeg Institute for Theoretical Physics, Winnipeg, Manitoba, Canada*
[c] *Instituto de Ciencias del Espacio (ICE, CSIC)*
C. Can Magrans s.n., 08193 Cerdanyola del Vallès, Catalonia, Spain
[d] *Institut d'Estudis Espacials de Catalunya (IEEC)*
08860 Castelldefels (Barcelona), Catalonia, Spain
[e] *Departament de Física Quàntica i Astrofísica and Institut de Ciències del Cosmos, Universitat de Barcelona, Martí i Franquès 1, 08028 Barcelona, Catalonia, Spain*
[f] *Institut d'Estudis Espacials de Catalunya (IEEC)*
08860 Castelldefels (Barcelona), Catalonia, Spain

E-mail: carrington@brandonu.ca, cristina.manuel@csic.es, soto@fqa.ub.edu

We calculate the real-time quantum chromodynamic (QCD) static potential in a high temperature medium, beyond the leading order Hard Thermal Loop (HTL) approximation, in the region where bound states transit from narrow resonances to wide ones. We find sizable contributions to both the real and the imaginary part of the potential. The calculation involves loop diagrams calculated in the HTL effective theory and power corrections to the QCD HTL Lagrangian. We compare our results with recent lattice data and check the consistency of different methods used in lattice calculations. We also discuss the usefulness of our results to guide lattice inputs.

10th International Conference on Quarks and Nuclear Physics (QNP2024)
8-12 July, 2024
Barcelona, Spain

*Speaker

PoS(QNP2024)109

1. Introduction. The zero temperature QCD static potential is Coulomb-like at short distances and linearly rising at long distances. At finite temperature the short-distance Coulomb-like potential becomes screened which leads to the idea that heavy quark-antiquark bound state production in Heavy Ion Collision (HIC) experiments will be suppressed through screening. However it turns out that another effect is more important. The static potential has an imaginary part that is bigger than the real part when the screening effects become large, which means that bound states disappear because they become wide resonances rather than because they are no longer supported by the Yukawa-like potential [1]. The suppression of heavy quark bound state production is observed in current HIC experiments in a pattern that is consistent with this idea. We calculate the real-time QCD static potential beyond leading order in a high temperature medium in the regime where bound states start melting. The calculation provides a check on the idea of ref. [1], which was based on the leading order results. Our results also give a wider set of physically motivated forms of the potential which can be used as an input for the Bayesian methods to extract the real-time static potential from Euclidean correlators calculated on the lattice.

The static potential is defined as the ground-state energy of a static quark and a static antiquark separated at a distance r. The calculation amounts to that of the expectation value of a rectangular Wilson loop with the length of the temporal sides of the loop taken to infinity. We work in the close-time-path formalism of thermal field theory and we use an approach based on HTL effective theory. The static quark and antiquark are (unthermalised) probe particles for which only the longitudinal photon (A_0) vertices in the time-ordered branch are relevant. We use the Coulomb gauge and dimensional regularization throughout, we use $C_F = (N_c^2 - 1)/(2N_c)$ where N_c is the number of colours, and g is the QCD coupling constant.

The leading order (LO) result for the momentum space potential, under the assumptions that $g \ll 1$ and the typical momentum exchange between the quark-antiquark satisfies $p \ll T$, is [1]

$$V_{1\text{lo}}(p) = g^2 C_F G(0,p) \qquad (1)$$
$$G(0,p) = -\frac{1}{m_D^2 + p^2} + \frac{i\pi T m_D^2}{p\left(m_D^2 + p^2\right)^2}$$

where $m_{=} gT\hat{m}_D$ is the Debye mass, with $\hat{m}_D = \sqrt{(N_c + N_f/2)/3}$, T is the temperature, N_f is the number of light flavors, and $G(p_0, p)$ the time-ordered longitudinal HTL propagator. The corresponding coordinate space potential is

$$V_{1\text{lo}}(r) = g^2 C_F \int \frac{d^3p}{(2\pi)^3}\, e^{i\vec{p}\cdot\vec{r}}\, G(0,\vec{p}) = -\frac{g^2 C_F}{4\pi\hat{r}}\left(m_D e^{-\hat{r}} - 2iT\, I_2(\hat{r})\right). \qquad (2)$$

We define the dimensionless integrals $I_j(\hat{r}) = \int_0^\infty d\hat{p}\, \sin(\hat{p}\hat{r})\, (\hat{p}^2+1)^{-j}$ and $\hat{r} \equiv r m_D$.

At any order in the loop expansion of the expression that defines the potential, we must decide if and how to dress the propagators and vertices in the resulting momentum integrals (i.e. if we should use bare n-point functions, or HTL corrected ones). This decision depends on the momentum scale that we choose to focus on, which in turn will determine the range of r where our coordinate space potential will be most reliable. To decide what momentum scale is important for our purposes we return to eq. (1). For a narrow resonance to exist the imaginary part of the static potential must be smaller than the real part. This implies that $p > (m_D^2 T)^{1/3} \sim g^{2/3} T$ or $p = g^a T$ with

$0 < a < 2/3$ (which we call semi-hard). The value $a = 2/3$ gives the momentum scale for which the real and imaginary parts of the leading order momentum space potential are the same size and is parametrically the scale at which we expect quarkonium to dissociate. We will take into account all corrections larger than g^2 to the real part and larger than g^{3a} and g^{2-a} to the imaginary part of the LO momentum space potential. Note that the scaling in a at LO is different for the real (g^{2-2a}/T^2) and the imaginary parts (g^{4-5a}/T^2). Two loop diagrams give corrections of order g^2 or smaller to the real part, and of order g^{3a} or smaller to the imaginary part. Including full HTL vertices in the self-energy diagrams gives corrections of order g^2 or smaller to the real part and of order g^{2-a} or smaller to the imaginary part. All together our conditions restrict a to be in the range $1/3 < a < 2/3$. The coordinate space potential that we obtain by Fourier transforming the momentum space potential will not be valid for $rm_D \gg 1$, since large r corresponds to momenta softer than the semi-hard scale we have chosen, or $rT \ll 1$, since small r corresponds to momenta larger than the temperature.

2. The static potential beyond leading order. The relevant diagrams are shown in fig. 1, where all the fermion lines do not depend on the spatial momenta (the static limit). There is one (4-dimensional) momentum variable that is integrated over (which we call k) and the momentum transfer is $p = (p_0, \vec{p})$. The fact that the semi-hard scale dominates the soft one means that HTL vertices and HTL propagators reduce to the bare ones up to corrections of order m_D^2/p^2. The gluon

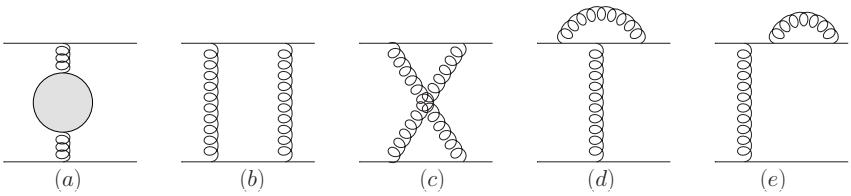

Figure 1: One-loop contributions to the static potential in the Coulomb gauge. All gluon lines correspond to longitudinal gluons. The iteration of the LO potential must be subtracted. Note that there is no diagram analogous to (d) with a three-gluon vertex.

self-energy bubble in fig. 1(a) at next-to-leading order in p/T is, for $p_0 \to 0$,

$$\Pi^{\rm ret}_{\rm nlo}(p_0, \vec{p}) = -\frac{g^2 T}{4}\left(N_c\left(p + i\,\frac{7}{3}\,\frac{p_0}{\pi}\right) - i\left(N_c - \frac{N_f}{2}\right)\frac{p_0\, p}{2\pi T}\right). \tag{3}$$

The first contribution comes from the loop with k semi-hard [2–4] and the second piece is the power correction. To find the corresponding contribution to the potential the result in (3) is used in the time ordered propagator. The leading contribution from the last four graphs in fig. 1 arises when the internal momentum $k \sim m_D$ and HTL propagators are used. The contribution from figs. 1(d,e) in momentum space is

$$V_2^{(\rm de)} = ig^4 N_c C_F G(0, p)\int \frac{d^4k}{(2\pi)^4}\,\frac{G(k_0, k)}{(k_0 + i\eta)^2}\,, \tag{4}$$

with $\eta \to 0^+$. To do the momentum integral we use time order propagators in the HTL limit and expand the Bose distribution since $k \sim m_D$. The contribution from the graphs in figs. 1(b,c) is

$$V_2^{(\rm bc)} = -\frac{ig^4 N_c C_F}{2}\int \frac{d^4k}{(2\pi)^4}\,\frac{G(k_0, \vec{k} + \vec{p})G(k_0, k)}{(k_0 + i\eta)^2}\,. \tag{5}$$

Since $p \gg (k, k_0)$ we can write under the integral sign

$$G(k_0, \vec{k} + \vec{p}) = G(0, p)\Big[1 - \frac{k^2}{3} G(0, p)\left(1 + 4m_D^2 G(0, p)\right)\Big] + O(\frac{m_D^3}{p^5}) \,. \tag{6}$$

To extend the range of r where our coordinate space potential will be valid, we keep m_D^2 in the denominators even though it is parametrically smaller than p^2. We call this the damped approximation. The coordinate space potential in the damped approximation is [5]

$$\begin{aligned} \mathrm{Re}[V_2] &= \frac{g^4 N_c C_F T}{64\pi^2 \hat{r}} \left\{ 8\left(I_2(\hat{r}) - I_1(\hat{r})\right) + \frac{e^{-\hat{r}}}{16}\left(3\pi^2 - 16 + \frac{\hat{r}}{6}\left(16 - \pi^2\right)\right)\right\} \\ i\mathrm{Im}[V_2] &= -i\frac{g^3 C_F T}{16\pi^2 \hat{m}_D}\left\{\frac{3\pi^2 - 16}{32\,\hat{r}} I_2(\hat{r}) + \frac{7}{3}\, N_c e^{-\hat{r}} - \frac{2g\hat{m}_D}{\pi\hat{r}}\left(N_c - \frac{N_f}{2}\right)\left(I_1(\hat{r}) - I_2(\hat{r})\right)\right\} . \end{aligned} \tag{7}$$

The first (second) line of the real (imaginary) part comes from fig. 1(a) and the remaining contributions from the last four diagrams in fig. 1.

We have not calculated contributions to potential from the soft region ($p \sim m_D$) because they would require full HTL propagators and vertices and are thus prohibitively difficult. However we can determine these contributions by taking advantage of the fact that they have a universal form in coordinate space at any order in g. To see this note that since we assume $rm_D \ll 1$ the exponential $e^{i\vec{p}\vec{r}}$ in the Fourier transform can be expanded in the soft region which gives

$$V_{\rm soft}(r) \;=\; \int \frac{d^3p}{(2\pi)^3}\left(1 + i\vec{p}\cdot\vec{r} - \frac{1}{2}(\vec{p}\cdot\vec{r})^2 + \cdots\right)\tilde{V}(p) \equiv V^0_{\rm soft} + V^2_{\rm soft}(r) + \cdots \,. \tag{8}$$

The second term is zero by symmetry in an isotropic system. The contribution from the soft momentum region thus reduces to a polynomial in r^2. At the order to which we work we need the zeroth order (the r-independent term) for the real part and up to the first order (the r^2 term) in the imaginary part [5]. The form of the soft contributions to the coordinate space potential is

$$V_{2,\rm soft} = g^4 q_0 T + i\left(g^3 i_0 T + g^5 i_2 r^2 T^3\right) , \tag{9}$$

where (q_0, i_0, i_2) are real constants. We will determine the values of the constants (q_0, i_0, i_2) by fitting to lattice data. We note that one can verify that (9) is the correct form for the soft contributions by expanding the NLO result in m_D/p and Fourier transforming the result. The coordinate space expression has poles of order $1/(d-3)$ that can be absorbed into the parameters of (9).

3. Comparison with lattice results. We consider bottomonium and take the mass of the bottom quark $m_b = 4676$ MeV. We fix g from the fit to the $T = 0$ lattice data for the static potential with $r \in [0, 0.3]$ fm which gives $g = 1.8$ and we use $N_c = N_f = 3$. First we compare our potential with [6]. The constants (q_0, i_0, i_2) are determined by fitting to the lattice data at values of r that satisfy $r > 0.04$ fm and $rm_D < 0.44$. To adjust the origin of energies we also add a temperature independent constant S to the real part of the potential. We also adjust the origin of energies for the LO potential and we plot results using $S_{\rm avg} = (S + S_{\rm lo})/2$. The values of the coefficients are given in the first row of table 1 and the potential is shown in fig. 2. For comparison we show in the second row of table 1 the parameters obtained by fitting to data points that satisfy 0.04 fm$< r <$ 0.3 fm [5]. The real part of the potential varies very little with temperature, in agreement with the data. For the

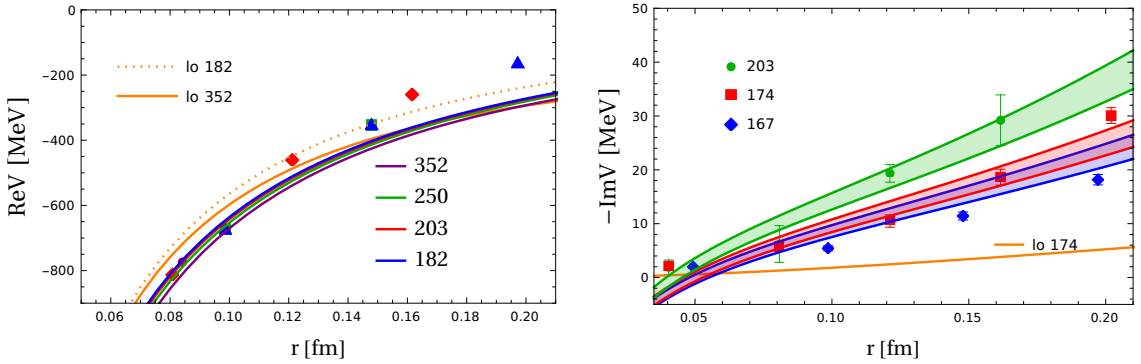

Figure 2: Real and imaginary part of V. The solid lines show $V = V_{1\text{lo}} + V_2 + V_{2,\text{soft}}$ in the damped approximation with parameters given in the text. The legends indicate the temperature in MeV. The LO contribution includes the one-loop static quark self-energies and for the imaginary part we show a single temperature since the remaining two would overlap with it. The solid bands on the lower plot indicate the uncertainty in the values of the fitted constants inherited from the error bars of the lattice data. Note that a slightly different fitting procedure is used in ref. [5] - see text for details.

imaginary part the soft contribution is mostly responsible for the large correction to the LO result.

To compare with the results of ref. [7] we solve the Schrödinger equation using our expression for the real part of the potential. To match the definition of [7], the widths for each temperature are obtained by calculating the expectation value $-\langle \text{Im}[V] \rangle$. The constants (q_0, i_0, i_2) are determined by fitting to the lattice data and their values are the third row in table 1 (the errors are obtained from the fits to the upper and lower values). The results are shown in fig. 3. The temperature dependence of both the binding energy and the decay width gives a reasonable description of the lattice data, and a considerable improvement with respect to the LO results.

We can use our results for the binding energies and widths to estimate the dissociation temperature, which we define as the temperature for which the energy difference to the threshold equals the thermal decay width $\Gamma = -2\langle \text{Im}[V] \rangle$. The results obtained from each set of fitted coefficients is given in the last column of table 1. For comparison the leading order result is $T_{\text{diss}} = 193.2$ MeV.

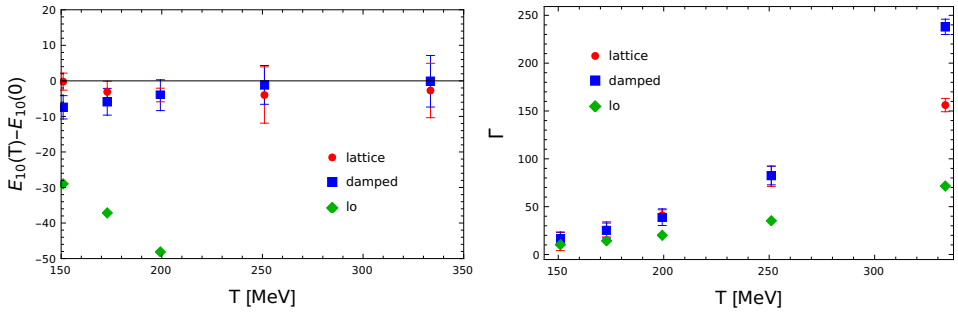

Figure 3: The temperature dependence of the binding energy and thermal width (in MeV) of the bottomonium ground state. The *lo* includes the one-loop static quark self-energies.

We have shown that our approach is able to reasonably describe the two sets of lattice data [6] and [7], but the parameter sets we need to do so are not entirely consistent. We believe this might be due to a problem in the extraction of the decay width in either lattice paper. Since all scales are

	q_0	i_0	i_2	S_{ave}	T_{diss}
[6]	0.019	-0.017± 0.001	0.13± 0.01	127.4 MeV	154.7 ± 4.7
[6]	0.027	-0.019 ± 0.001	0.194 ± 0.002	209.5 MeV	142.7 ± 1.1
[7]	0.044± 0.002	-0.026 ± 0.009	0.052± 0.002	-	202 ± 10

Table 1: Fitted coefficients and the corresponding dissociation temperature. The first row corresponds to the fitting procedure used to produce fig. 2 and the second row is the procedure of ref. [5].

explicit in our approach, we expect that the fitted numerical coefficients should be approximately the same size. This is true except for the values of i_2 obtained by fitting to the data of [6]. The corresponding dissociation temperature is also very low, incompatible with earlier lattice studies that indicate it is much higher than the crossover temperature.

4. Summary and conclusions. We have calculated the momentum space potential including corrections beyond the leading order HTL result for typical momentum transfer p that satisfies $m_D \ll p \ll T$. This is the relevant region to obtain the dissociation temperature for heavy quarkonium. We have extended our calculation to softer p by keeping suitable $p^2 + m_D^2$ terms unexpanded. The Fourier transform gives the coordinate space potential for $1/T \ll r \ll 1/m_D$ up to a polynomial in r^2 which encodes the contribution for $p \lesssim m_D$ at any order in g. We expect our expressions (7,8,9) will give a reasonable approximation at larger r as well, since explicit damping factors are kept. Our results therefore provide useful inputs for the Bayesian methods required in the effort to determine the real-time static potential from lattice QCD. As an example, we have shown that our results describe reasonable well two different sets of lattice data, whereas the LO result fails to do so. We have also been able to identify an inconsistency between these two sets of data. This is not surprising because of the notorious difficulty of extracting the imaginary part of the potential in lattice calculations. Our results could be used as a check when comparing the validity of different lattice methods.

Acknowledgments. We thank Peter Petreczky and Rasmus Larsen for providing the data of Refs. [7] and [6], respectively. MEC acknowledges support by the Natural Sciences and Engineering Research Council of Canada under grant SAPIN-2023-00023 and thanks ICCUB and ICE for hospitality. CM was supported by Ministerio de Ciencia, Investigación y Universidades (Spain) MCIN/AEI/10.13039/501100011033/ FEDER, UE, under the project PID2022-139427NB-I00, by Generalitat de Catalunya by the project 2021-SGR-171 (Catalonia), and also partly supported by the Spanish program Unidad de Excelencia Maria de Maeztu CEX2020-001058-M, financed by MCIN/AEI/10.13039/501100011033. JS acknowledges financial support from Grant No. 2017-SGR-929 and 2021-SGR-249 from the Generalitat de Catalunya and from projects No. PID2022-136224NB-C21, PID2022-139427NB-I00 and No. CEX2019-000918-M from Ministerio de Ciencia, Innovación y Universidades.

References

[1] M. Laine, O. Philipsen, P. Romatschke and M. Tassler, *Real-time static potential in hot QCD*, *JHEP* **03**, 054 (2007) [hep-ph/0611300].

[2] A. K. Rebhan, *The NonAbelian Debye mass at next-to-leading order,* Phys. Rev. D **48**, R3967 (1993) [hep-ph/9308232].

[3] C. Y. Shi, J. Q. Zhu, Z. L. Ma and Y. D. Li, *Thermal Width for Heavy Quarkonium in the Static Limit*, Chin. Phys. Lett. **32**, 121201, (2015).

[4] J. Q. Zhu, Z. L. Ma, C. Y. Shi and Y. D. Li, *Thermal single-gluon exchange potential for heavy quarkonium in the static limit*, Nucl. Phys. A **942**, 54 (2015).

[5] M. E. Carrington, C. Manuel and J. Soto, *The high temperature QCD static potential beyond leading order*, [hep-ph/2407.00310].

[6] A. Bazavov, D. Hoying, O. Kaczmarek, R. N. Larsen, S. Mukherjee, P. Petreczky, A. Rothkopf and J. H. Weber, *Un-screened forces in Quark-Gluon Plasma?*, [hep-lat/2308.16587].

[7] R. Larsen, S. Meinel, S. Mukherjee and P. Petreczky, *Excited bottomonia in quark-gluon plasma from lattice QCD*, Phys. Lett. B **800**, 135119 (2020) [hep-lat/1910.07374].

PoS(QNP2024)109